Published online 16 March 2008

Nucleic Acids Research, 2008, Vol. 36, No. 8 ***2667–2676***
doi:10.1093/nar/gkn119

Autoregulation of the *Escherichia coli melR* promoter: repression involves four molecules of MelR

Shivanthi Samarasinghe[1], Mohamed Samir El-Robh[1], David C. Grainger[1], Wenke Zhang[2], Panos Soultanas[2] and Stephen J. W. Busby[1,*]

[1]School of Biosciences, The University of Birmingham, Edgbaston, Birmingham B15 2TT and [2]The University of Nottingham, Centre for Biomolecular Sciences, University Park, Nottingham NG7 2RD, UK

Received December 20, 2007; Revised February 29, 2008; Accepted March 3, 2008

ABSTRACT

The *Escherichia coli* MelR protein is a transcription activator that autoregulates its own promoter by repressing transcription initiation. Optimal repression requires MelR binding to a site that overlaps the *melR* transcription start point and to upstream sites. In this work, we have investigated the different determinants needed for optimal repression and their spatial requirements. We show that repression requires a complex involving four DNA-bound MelR molecules, and that the global CRP regulator plays little or no role.

INTRODUCTION

Repressors play an important role in the complex web of regulatory interactions that control transcription in *Escherichia coli*. Many repressors bind to sites that overlap key promoter elements and down-regulate promoter activity by preventing the binding of RNA polymerase (1). At some promoters, efficient down-regulation requires the repressor to be bound at tandem operators. In a number of instances, these operators are separated by more than 100 bp and it has been suggested that bound repressors interact, forming a repression loop in the intervening DNA (2,3). One of the best-studied examples is the AraC protein, an arabinose-trigerred transcription factor (4). In the absence of arabinose, transcription of the *araC* gene is repressed by two AraC molecules that bind to two DNA sites (*O2* and *I1*) that flank the *araC* promoter and are separated by 210 bp (5). In this paper, we present a study of similar complex repression by a transcription factor that is related to AraC, the *E. coli* K-12 MelR protein, which represses transcription of its own gene, *melR*.

MelR is a member of the AraC-XylS family of bacterial gene regulatory proteins (6) and our previous studies have shown that MelR, together with the cyclic AMP receptor protein, CRP, regulates expression of the *melAB* operon that encodes products essential for melibiose metabolism (7). Melibiose triggers the formation of an activatory complex of four MelR molecules and one CRP dimer at the *melAB* promoter (8,9). In this complex, MelR binds to two pairs of DNA sites, sites 2 and 2′ and sites 1 and 1′, and CRP binds between the two pairs of sites (Figure 1A). This complex cannot form in the absence of melibiose because MelR, whilst binding to sites 2, 1 and 1′, is unable to occupy site 2′.

Expression of MelR is controlled by the *melR* promoter, which drives initiation of a divergent transcript from 237-bp upstream of the *melAB* transcript start point (10,11). Transcription of *melR* is completely dependent on cAMP-CRP binding to a DNA target that overlaps the promoter -35 region, and is autoregulated by MelR binding to a fifth target site, site R, that overlaps the *melR* promoter transcript start (Figure 1A). Like many members of the AraC-XylS family, MelR consists of an N-terminal ligand-binding domain connected, via a flexible linker, to an ~100 amino acid C-terminal DNA-binding domain (12,13). The DNA-binding domain, that is the defining feature of all AraC-XylS family regulators (6,14), contains two helix–turn–helix motifs which, when bound at operator targets, recognize different base sequences in adjacent major grooves in a specific orientation (15). The orientation of MelR binding at sites 2 and 2′ and sites 1 and 1′ has already been determined experimentally (16) and here we have investigated the orientation of MelR bound at site R.

Previously, we found that optimal MelR-dependent repression of the *melR* promoter occurs in the absence of melibiose, and requires MelR-binding site 2, centred between base pairs −174 and −175 (i.e. position

*To whom correspondence should be addressed. Tel: (+44) 121 414 5439; Fax: (+44) 121 414 5925; Email: s.j.w.busby@bham.ac.uk

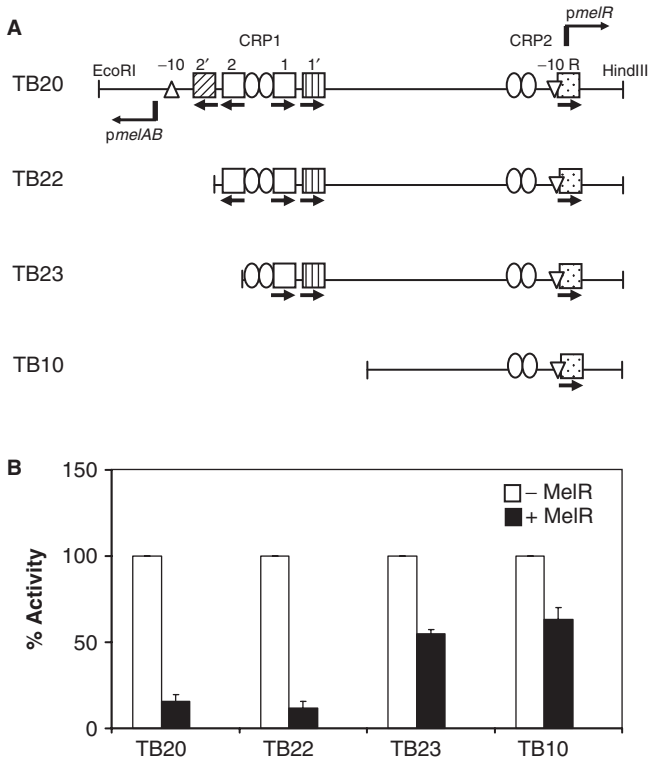

Figure 1. The *melR* promoter and its repression by MelR. (**A**) The figure illustrates the starting TB20 EcoRI–HindIII fragment carrying the *mel* operon regulatory region together with the TB22, TB23 and TB10 derivatives. Bent arrows indicate the transcription start sites for the *melAB* and *melR* promoters and triangles denote the corresponding −10 hexamer elements. The locations of the different 18-bp DNA sites for MelR are indicated by squares, with their orientation shown by horizontal arrows. The two DNA sites for CRP, CRP1 and CRP2, are denoted by pairs of ovals. (**B**) The figure illustrates β-galactosidase expression in *E. coli* WAM1321 cells carrying *melR* promoter::*lac* fusions, encoded by pRW50 with insertions of the TB20, TB22, TB23 or TB10 EcoRI–HindIII fragments, as indicated. β-Galactosidase expression was measured in cells containing pJW15 that encodes MelR (+MelR: black filled bars) or the control pJW*ΔmelR* with no *melR* insert (−MelR: open bars). For each promoter, the activity +MelR is expressed as a % of the activity −MelR (300, 350, 300 and 330 Miller units for TB20, TB22, TB23 and TB10, respectively). The results are averages from at least three independent determinations.

−174.5), upstream of the *melR* transcript start point (17). By analogy with the action of AraC at the *araC* promoter, it was suggested that repression might simply be due to loop formation between two MelR molecules bound at site R and site 2 (17). Hence, in this work, we used *in vivo* and *in vitro* methods to investigate the determinants needed for MelR-dependent repression of the *melR* promoter. We show that the simple looping model is not applicable and that repression involves four bound MelR molecules, and we argue for a repression complex rather than a repression loop.

MATERIALS AND METHODS

Strains, plasmids and promoters

In this work, we used the WAM1321 Δ*lac* Δ*melR* Δ*melA* strain of *E. coli* K-12 (13). The starting point was the EcoRI–HindIII TB20 fragment carrying the *E. coli mel* operon regulatory region, described by Kahramanoglou *et al.* (13), illustrated in Figure 1A, together with the shorter TB10 derivative that lacks sequences upstream of the *melR* promoter. Derivatives of the TB20 fragment are illustrated in the figures and the complete base sequence of each fragment from the EcoRI site to the HindIII site is shown in Figure 1 of the online Supplementary Data. All DNA sequences were checked by the University of Birmingham Functional Genomics Service (http://www.genomics.bham.ac.uk/). By convention, in this paper, sequences are numbered with respect to the transcription start point of the *melR* promoter with upstream and downstream locations denoted by minus and plus prefixes, respectively. EcoRI–HindIII fragments carrying the *melR* promoter were cloned into pRW50, a broad host range low copy number *lac* expression vector (18), to create *melR* promoter::*lac* fusions. Plasmid pRW50 and derivatives were maintained in host strains with 35 μg/ml tetracycline. Experiments to measure effects of MelR *in vivo* used pJW15, which carries the wild-type *melR* gene, and an empty control pJW15Δ*melR* (13,19). Plasmid pJW15 and derivatives were maintained in host strains with 80-μg/ml ampicillin. The derivative of pJW15 encoding Val273 MelR is described in Grainger *et al.* (20). For *in vitro* experiments, *melR* promoter fragments were cloned into plasmid pSR that was maintained in host strains with 80-μg/ml ampicillin (21).

Construction of promoter fragments

Different promoter fragments were constructed by using PCR or megaprimer PCR (22). Table 1 of the online Supplementary Data lists the base sequence of all the oligo primers that were used in these constructions.

Starting with the TB20 fragment cloned in pSR, PCR was used to construct the shorter TB22 and T23 fragments using primers D51247 and D21970 for TB22, and D51248 and D21970 for TB23. The TB20 5C, 13G and 13T derivatives were constructed by megaprimer PCR using primers D21970 together with D47376, D47377 and D47378, respectively. Corresponding products were then used as megaprimers together with primer D31961 to amplify the full-length TB20 mutated fragment. The TB210 fragment was constructed from a megaprimer made with D48803 and D21970 which was then used in conjunction with D31961 to give TB20 with a consensus *melR* promoter −10 hexamer element. TB211 was then derived from TB210 using D49453 and D21970 to make a megaprimer, which was then used together with D31961. Finally, TB201 and TB222 were derived from TB20 and TB211, respectively, using D50812 and D21970 to generate megaprimers. These were then used in combination with D31961 to generate the mutant TB201 and TB222 fragments.

Starting with the TB22 fragment cloned in pSR, the Δ5 derivative was constructed using PCR. To do this, upstream EcoRI–NcoI and downstream NcoI–HindIII fragments were generated using primers D31961 and D55280 and D55278 and D21970, respectively and ligated together. For the Δ10-derivative, the same upstream

EcoRI–NcoI fragment was used together with a downstream NcoI–HindIII fragment generated using primers D21970 and D55274. For the +5 derivative, the same D31961/D55280 EcoRI–NcoI fragment was used together with a downstream NcoI–HindIII fragment generated using primers D21970 and D55276. To make the +41 and +91 inserts, first a derivative of TB22 carrying NcoI and SalI sites downstream of site 1′ was constructed. To do this, a megaprimer was made using D56893 and D21970. The megaprimer was then used as a primer together with D31961 to generate the TB22 derivative. The TB22 + 41 and TB22 + 91 fragments were then constructed by insertion of blocks of sequence amplified from pBR322 and cloned as NcoI–SalI fragments. These fragments were generated after PCR using D56890 and D56891 (for +41) or D56892 (for +91). The TB28 fragment was generated by ligating upstream EcoRI–NcoI and downstream NcoI–HindIII fragments together. The upstream fragment was generated using primers D31961 and D58647 with TB22 cloned in pSR as a template. The downstream fragment was generated using primers D58648 and D21970 with TB22 + 91 cloned in pSR as a template.

Measurement of promoter activities *in vivo*

Assays were performed in WAM1321 Δ*lac* Δ*melR* Δ*melA* cells containing *melR* promoter::*lac* fusions on pRW50 derivatives, into which the different fragments carrying the *melR* promoter had been cloned. The cells also carried pJW15 encoding wild-type or mutant *melR*, or the control 'empty' vector plasmid, pJW*ΔmelR*, with no *melR* insert. Note that, in pJW15, *melR* is transcribed from the *melR* promoter, but that the upstream limit of *melR* promoter sequence is at position –59 upstream of the *melR* promoter transcript start (11,19). Thus, the *melR* promoter is not efficiently repressed by MelR, and MelR is over-expressed. Cells were grown in minimal medium, with fructose as a carbon source, as in our previous work (10), and the Miller method (23) was used to quantify β-galactosidase expression.

Purification and labelling of MelR for Fe-BABE experiments

MelR carrying a single cysteine at residue 269 was over-expressed, purified and labelled with Fe-BABE, and used in footprinting experiments, exactly as described by Grainger *et al.* (16). ^{32}P end-labelled DNA fragments were used at a final concentration of 10 nM in buffer containing 60 mM HEPES, pH 8.0, 1.25 μM potassium glutamate and 40 μg/ml herring sperm DNA. Incubations contained 0.75 μM labelled MelR, 75 nM CRP and 200 μM cyclic AMP.

In vitro transcription, DNAase I footprinting and electromobility shift assays

These experiments were performed as described by Belyaeva *et al.* (8) using MelR purified by the method of Caswell *et al.* (24). For *in vitro* transcription experiments, caesium chloride purified supercoiled pSR plasmid carrying the TB22 or TB23 EcoRI–HindIII *melR* promoter inserts was used. Ten-nanomolar template was pre-incubated with purified CRP (200 nM; gift from Dr Georgina Lloyd) and cAMP (200 μM) and purified *E. coli* holo RNA polymerase (20 nM; purchased from Epicentre Biotechnologies, Madison) in 40 mM Tris–acetate pH 7.9, 10 mM $MgCl_2$, 1 mM DTT, 100 mM KCl and 50 μg/ml BSA, either with or without 100 nM purified MelR. Transcription was started with the addition of 200 μM ATP, CTP and GTP, 10 μM α^{32}P-labelled UTP and 100 μg/ml heparin and labelled RNA products were analysed on sequence gels. Transcripts were quantified using ImageQuant software.

For electromobilty shift assays, we used EcoRI–HindIII fragments that had been purified from pSR carrying the TB22 or TB28 inserts and end-labelled with γ^{32}P ATP at the HindIII end (19). For DNAase I footprinting, we used AatII–HindIII fragments that had been purified from pSR, carrying the TB22 or TB28 EcoRI–HindIII inserts, and end-labelled with γ^{32}P ATP at the HindIII end. Different concentrations of MelR were pre-incubated for 5 min at 37°C with 4 nM of the DNA fragment in buffer containing 20 mM HEPES pH 8.0, 5 mM $MgCl_2$, 50 mM potassium glutamate, 1 mM DTT, 0.5 mg/ml BSA and 0.05 mg/ml herring sperm DNA. Samples were treated with 3 μl of DNAase I (0.15×10^{-3} U/μl) for 5 min at 37°C and reactions were quenched with 10 vol of stop solution (0.3 M sodium acetate pH 5.2 and 10 mM EDTA). After phenol–chloroform treatment and ethanol precipitation, samples were re-suspended in gel-loading buffer (40% deionized formamide, 5 M urea, 5 mM NaOH, 1 mM EDTA, 0.025% bromophenol blue and 0.025% xylene cyanole), heated for 2 min at 90°C and then loaded on a 6% polyacrylamide sequencing gel. Footprints were scanned and quantified using Bio-Rad Quantity One software. To compare the affinity of MelR for site R in the TB22 and TB28 fragments, we measured the intensity of bands which result from cleavage at three different positions in site R, where cleavage is reduced by MelR binding. Intensities were measured in footprints obtained at different MelR concentrations, and lane-to-lane variation was accounted for by normalization to the intensities of bands at positions -35 and -65, that are unaffected by MelR binding. Comparison of the apparent concentration of MelR required for 50% protection at site R in the two fragments gives an estimate of relative binding affinities.

Atomic force microscopy (AFM) of MelR–DNA complexes

The DNA fragment used was generated by digestion of pSR carrying the TB22 EcoRI–HindIII fragment with SspI and NdeI. The fragment was purified using a Qiagen gel extraction kit and was eluted with 8 mM Tris–HCl, pH 8.5. MelR protein, purified by the Caswell method (24), was dialysed into buffer containing 50 mM Tris pH 7.6 and 600 mM NaCl, and complexes were formed by incubating 25 nM DNA fragment and 1 nM MelR in buffer containing 40 mM Tris pH 8.0, 0.1 M KCl, 50 mM NaCl and 0.5 mM EDTA for 10 min at room temperature. Samples (10 μl) were then deposited onto a freshly cleaved mica disk that had been treated with 2 mM $NiCl_2$ (25). After incubation for 30 s, the surface was slowly rinsed with water and then allowed to dry under a gentle flow of nitrogen gas. Imaging was carried out with a Digital

Instruments Nanoscope IIIa Mutlimode AFM with a type E scanner (Veeco, Santa Barbara, CA, USA) in tapping mode. The cantilevers used were silicon-tapping probes with a spring constant of 34.4–74.2 N/m (Olympus, OMCL-AC160TS). The tapping set point was adjusted to minimize probe–sample interactions.

RESULTS

Measurement of *melR* promoter activity: repression by MelR

The starting point of this work was the TB20 EcoRI–HindIII fragment that covers the intergenic region between the divergent *E. coli melR* and *melA* genes and the translation start points. This fragment, together with the TB22, TB23 and TB10 truncated derivatives (Figure 1A), was cloned into pRW50, a *lac* expression vector, to generate *melR* promoter::*lac* fusions. To measure MelR-dependent repression of *melR* promoter activity, the pRW50 derivatives carrying the TB20, TB22, TB23 or TB10 fragments were transformed into WAM1321 Δ*melR* Δ*lac* cells containing either pJW15, encoding *melR*, or empty control vector, pJWΔ*melR* and β-galactosidase activities were measured. The results, illustrated in Figure 1B, show that, with the TB20 fragment cloned in pRW50, MelR causes a >5-fold reduction in β-galactosidase expression. Similar repression is seen with the TB22 fragment, in which *melAB* promoter sequences upstream of MelR-binding site 2 have been removed. In contrast, and in full agreement with the previous results of Wade *et al.* (17), the longer deletion in the TB23 fragment, that removes MelR binding site 2, results in a sharp reduction in the repression of the *melR* promoter by MelR. This reduced repression is unchanged by the longer deletion in the TB10 fragment.

Next, we attempted to reproduce MelR-dependent repression of the *melR* promoter *in vitro*. To do this, the TB22 and TB23 fragments were cloned into plasmid pSR such that the *melR* promoter was placed upstream of the bacteriophage λ *oop* factor-independent terminator. The recombinant plasmids were incubated with purified RNA polymerase holoenzyme and the activator, CRP, and radiolabelled nucleoside triphosphates were added. Analysis of the RNA products, shows that two discrete RNA species were produced (Figure 2). These correspond to the plasmid-encoded RNA-1 (108 nt) and a longer 138 base transcript that initiates at the *melR* promoter and runs to the *oop* terminator. Note that the production of the 138 base RNA, but not RNA-1, is dependent on the inclusion of CRP in the assay (control experiments not shown). The experiment illustrated in Figure 2 shows that MelR has little or no effect on the synthesis of RNA-1 but represses synthesis of the transcript from the *melR* promoter. In accord with the *in vivo* assays (Figure 1B), repression is greater with the TB22 template, which includes MelR-binding site 2, than with the TB23 template.

Orientation of MelR bound at site R

Wade *et al.* (17) showed that MelR-binding site R is essential for MelR-dependent repression of the *melR* promoter, and Figure 3A shows the proposed 18-bp binding sequence compared to the consensus (7). In another study (16), it was found that base pairs 5 and 13 of the consensus sequence make important contacts with the side chains of amino acids N222 and R273, respectively, in the first and second helix–turn–helix motifs of the MelR DNA-binding domain. To confirm the location of site R and its orientation, three derivatives of the TB20 fragment, carrying base substitutions at position 5 or position 13 of the proposed site R sequence, were constructed (Figure 3A). MelR-dependent repression of the *melR* promoter carried by each derivative was then measured, as above. Results illustrated in Figure 3B show that the 5C substitution, which removes the consensus G base at position 5, reduced MelR-dependent repression. Furthermore, though the base at position 13 is the non-consensus A, substitution with a T also reduces MelR-dependent repression. In contrast, MelR-dependent repression is enhanced by the 13G change which introduces a consensus G.

To determine experimentally the orientation of MelR bound at site R we used complementary genetic and

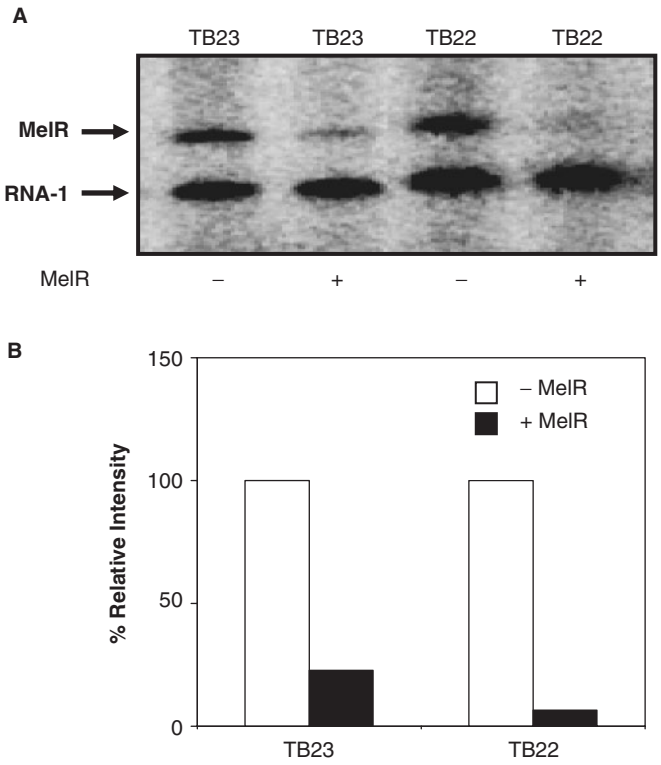

Figure 2. *In vitro* transcription at the *melR* promoter. (**A**) The figure shows an autoradiogram on which ^{32}P-labelled RNA synthesized *in vitro* was analysed. RNA was made using purified *E. coli* RNA polymerase holoenzyme to transcribe purified pSR plasmid carrying either the TB22 or TB23 *melR* promoter inserts (Figure 1A). Incubations were performed with or without 100 nM purified MelR, as indicated. Bands corresponding to the plasmid-encoded 108 base RNA-1 transcript and the 138 base transcript starting at the *melR* promoter are indicated. (**B**) The bars illustrate measurements of the *melR* transcript normalized to RNA-1. For TB22 and TB23, the amount of transcript +MelR is expressed as a % of the amount of transcript −MelR. The results are averages from three independent determinations.

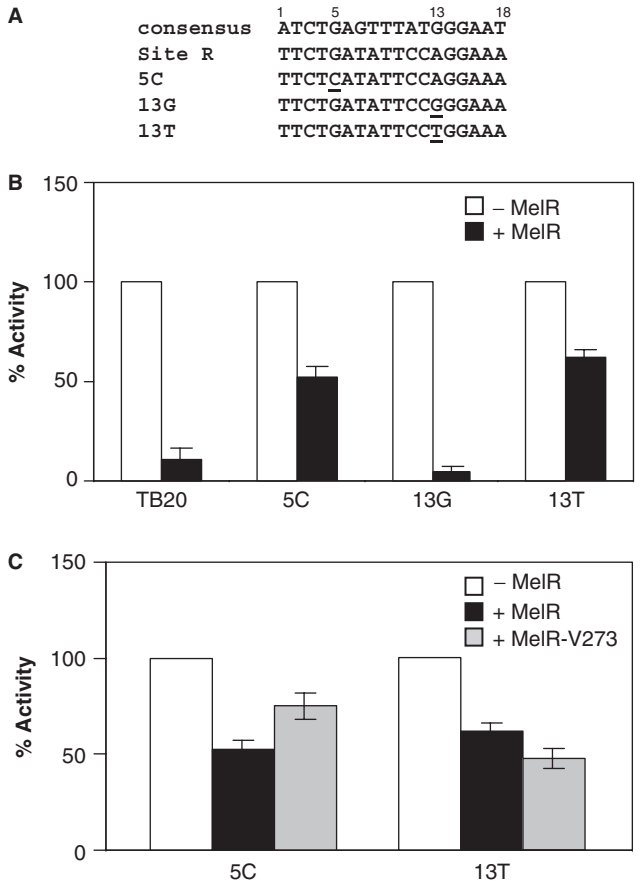

Figure 3. Mutational analysis of site R at the *melR* promoter. (**A**) The figure shows an alignment of the consensus 18-bp DNA site for MelR, found at site 1 and site 2, with the proposed sequence of MelR-binding site R at the *melR* promoter. Bases are numbered according to the orientations shown in Figure 1A. The sequences of site R carrying the 5C, 13G and 13T mutations, which were made in the TB20 fragment, are also indicated. Base changes are highlighted by underlining. (**B**) The figure illustrates β-galactosidase expression in *E. coli* WAM1321 cells containing *melR* promoter::*lac* fusions, encoded by pRW50 carrying the wild-type TB20 EcoRI–HindIII fragment, or the 5C, 13G or 13T derivatives, as indicated. β-Galactosidase expression was measured in cells containing pJW15 that encodes MelR (+MelR: black filled bars), or the control pJW*ΔmelR* with no *melR* insert (−MelR: open bars). For each promoter, the activity +MelR is expressed as a % of the activity −MelR (300, 400, 440 and 120 Miller units for TB20 and the 5C, 13G or 13T derivatives, respectively). The results are averages from at least three independent determinations. (**C**) The figure illustrates β-galactosidase expression in *E. coli* WAM1321 cells containing *melR* promoter::*lac* fusions, encoded by pRW50 carrying the 5C or 13T derivatives of the EcoRI–HindIII TB20 fragment as indicated. β-Galactosidase expression was measured in cells containing pJW15 that encodes wild-type MelR (+MelR: black filled bars), pJW15 that encodes Val273 MelR (+MelR-V273: grey filled bars) or the control pJW*ΔmelR* with no *melR* insert (–MelR: open bars). For each promoter, the activity +MelR is expressed as a % of the activity –MelR. Results are averages from six independent determinations.

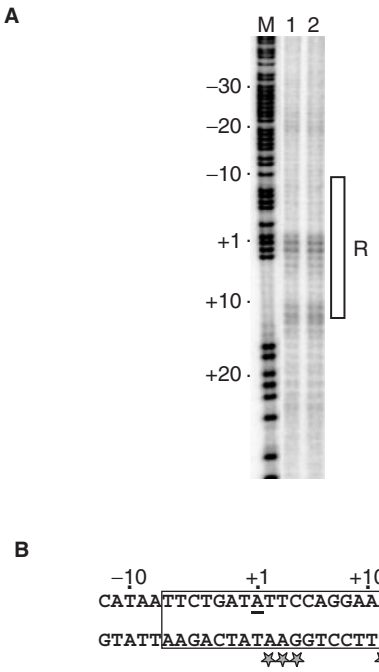

Figure 4. Binding of Fe-BABE-labelled MelR to *melR* promoter DNA. (**A**) The figure shows an autoradiogram of a segment of a sequencing gel that analyses DNA cleavage at MelR-binding site R, resulting from hydroxyl radicals generated by Fe-BABE attached to residue 269 of purified MelR. For this experiment, 0.75 μM of MelR labelled with Fe-BABE was incubated with 10-nM DNA fragment, either without (lane 1) or with (lane 2) 10 mM melibiose (see Materials and methods section). The DNA fragment was purified from a restriction digest of plasmid pSR carrying the TB10 *melR* promoter fragment and end-labelled at the HindIII site downstream of the *melR* promoter. The gel was calibrated with a Maxam–Gilbert G+A reaction (lane M). The location of MelR-binding site R is shown by vertical box and calibrations correspond to positions with respect to the *melR* transcript start point. (**B**) The figure shows the base sequence around the *melR* transcript start point (+1). The locations of DNA cleavage, resulting from hydroxyl radicals generated by Fe-ABE attached to residue 269 of MelR are indicated by stars. The 18-bp MelR-binding site R is enclosed by a box.

biochemical approaches. First, we exploited the observation that the RV273 substitution in helix–turn–helix 2, permits MelR to recognize binding targets with a T at position 13 (20). Results in Figure 3C show that Val273 MelR gives a small enhancement in repression of the *melR* promoter carrying the 13T substitution in site R, compared to wild-type MelR. In contrast, repression of the 5C derivative is reduced with Val273 MelR. These data are consistent with a model in which helix–turn–helix 2 of MelR contacts the downstream part of site R, with residue 273 interacting with the base pair at position 13. To confirm this, we used a preparation of purified MelR that had been labelled with an inorganic DNA cleavage reagent at residue 269, adjacent to helix–turn–helix 2 (16). The reagent, *p*-bromoacetamidobenzyl-EDTA-Fe (Fe-BABE), generates a pulse of hydroxyl radicals that can be used to find the location of DNA binding of a protein and its orientation (26–28), and previously we exploited this to determine the orientation of MelR binding at sites 1′, 1, 2 and 2′ (16). Figure 4A shows the pattern of DNA cleavage due to Fe-BABE covalently attached at residue 269 of purified MelR, bound at site R. As expected, two sets of bands are observed. These result from cleavage at minor grooves on either side of the site where helix–turn–helix 2 is bound, which occurs as a pulse of hydroxyl radicals encounters the neighbouring DNA. Figure 4B shows the location of these sites of cleavage

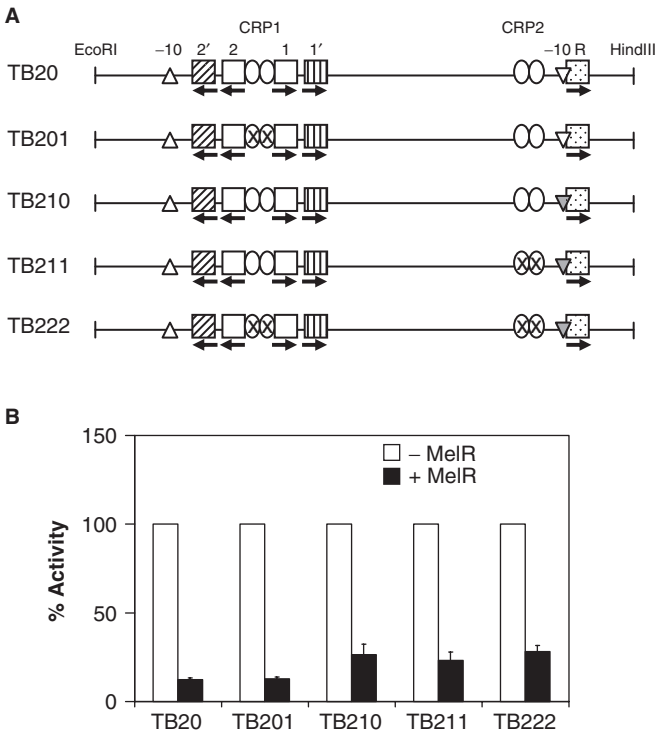

Figure 5. Mutations in CRP sites do not affect repression of the *melR* promoter. (**A**) The figure illustrates the starting TB20 EcoRI–HindIII fragment carrying the *mel* operon regulatory region, together with the TB201, TB210, TB211 and TB222 derivatives. The locations of the different 18-bp DNA sites for MelR are indicated by squares with their orientations shown by horizontal arrows. The two DNA sites for CRP, CRP1 and CRP2, are denoted by pairs of ovals and inactivation of these sites is denoted by crosses, which denote changes at positions 7 and 16 of each 22-bp site (9). Triangles denote the −10 hexamers of the *melAB* and *melR* promoters. Shaded triangles in the TB210, TB211 and TB222 derivatives denote mutation of the *melR* promoter −10 hexamer from 5′ CATAAT 3′ to 5′ TATAAT 3′. (**B**) The figure illustrates β-galactosidase expression in *E. coli* WAM1321 cells carrying *melR* promoter::*lac* fusions, encoded by pRW50 with insertions of the TB20, TB201, TB210, TB211 or TB222 EcoRI–HindIII fragments as indicated. β-Galactosidase expression was measured in cells containing pJW15 that encodes MelR (+MelR: black filled bars), or the control pJW*ΔmelR* with no *melR* insert (−MelR: open bars). For each promoter, the activity +MelR is expressed as a % of the activity −MelR (300, 260, 560, 400 and 390 Miller units for TB20, TB201, TB210, TB211 and TB222, respectively). The results are averages from at least three independent determinations.

in the context of MelR-binding site R. The results confirm that helix—turn–helix 2 of MelR binds to the downstream half of site R and hence MelR must bind in opposite orientations at site R and site 2 (Figure 1A).

CRP is not needed for MelR-dependent repression of the *melR* promoter

To investigate the possibility that the activator CRP is required for repression of the *melR* promoter by MelR, we constructed derivatives of the TB20 fragment carrying mutations that inactivated either or both DNA sites for CRP, and measured MelR-dependent repression (Figure 5A). Thus, TB201 is a derivative of TB20 in which the DNA site for CRP located between MelR site 1 and site 2 (CRP1) is inactivated. Results illustrated in Figure 5B show that MelR-dependent repression of the *melR* promoter is unaffected when CRP binding at this target is prevented. It is more complicated to investigate the DNA site for CRP located 41-bp upstream of the *melR* transcript startpoint (CRP2) because its inactivation leads to loss of *melR* promoter activity (11). Hence, we constructed the TB210 fragment, in which the *melR* promoter –10 hexamer element was changed from 5′ CATAAT 3′ to the consensus 5′ TATAAT 3′. This change confers partial CRP independence on the *melR* promoter (data not shown) and also causes a small reduction in MelR-dependent repression. We then constructed the TB211 fragment in which the CRP2 site was inactivated, and TB222, in which both DNA sites for CRP were inactivated (Figure 5A). Results illustrated in Figure 5B show that the MelR-dependent repression of the *melR* promoter in the TB210 fragment is unchanged in the TB211 and TB222 derivatives. This indicates that CRP binding plays little or no role in MelR-dependent repression of the *melR* promoter.

Other determinants for MelR-dependent repression of the *melR* promoter

To investigate the effects of altering the spacing between MelR-binding site R and the upstream sites, derivatives of the TB22 fragment with 5- or 10-bp deletions, or with 5-, 41- or 91-bp insertions were constructed (see Figure 6A and Materials and methods section). MelR-dependent repression of the *melR* promoter in each of the new constructs was measured as above and the results are illustrated in Figure 6B. The data show that repression is reduced by deletion of 5 bp but is restored in the 10-bp deletion construct. Similarly, repression is reduced by insertion of 5 bp but is restored, at least partially, by the 41- or 91-bp insertions. In our previous study (17), we reported that repression of the *melR* promoter by MelR was unaffected by point mutations in either site 1 or site 1′. However, it was subsequently found that, whilst these point mutations weakened MelR binding at these targets, their occupation by MelR was not prevented (Mohamed El-Robh, unpublished results). Hence, the TB28 fragment, in which both site 1 and site 1′ were replaced by unrelated sequence, was constructed (see Figure 6A and Materials and methods section). Results illustrated in Figure 6B show that MelR-dependent repression of the *melR* promoter in the TB28 fragment is reduced. This suggests that occupation of sites 1 and 1′ by MelR plays a role in repression.

In vitro studies of MelR binding at the *melR* promoter

Our results show that MelR-dependent repression of the *melR* promoter is contingent on MelR binding to site R and is somehow modulated by MelR binding to upstream sites 2, 1 and 1′. Hence an electromobility shift assay (Figure 7) and a DNAase I footprinting experiment (Figure 8) were used to investigate the occupation of the different binding sites at the TB22 and TB28 promoters by purified MelR.

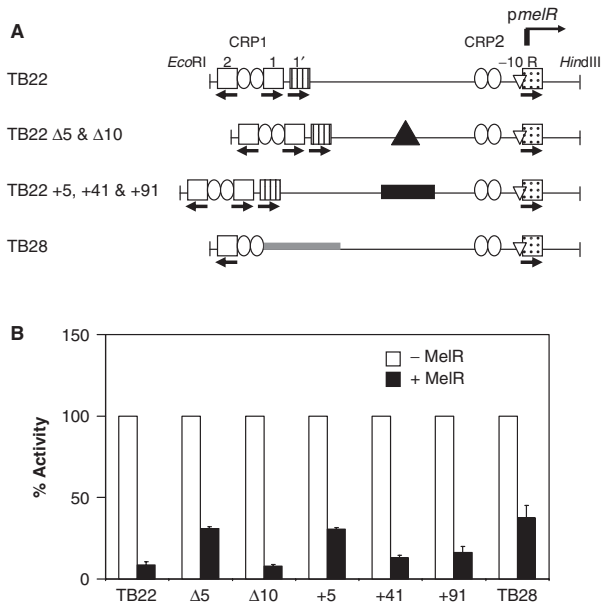

Figure 6. Insertions and deletions between site 2 and site R at the *melR* promoter. (**A**) The figure illustrates the starting TB22 EcoRI–HindIII fragment carrying the *melR* promoter, together with different derivatives. The bent arrow indicates the transcription start point for the *melR* promoter and open triangles denote the −10 hexamer element. The locations of different 18-bp DNA sites for MelR are indicated by squares, with their orientation shown by horizontal arrows. The two DNA sites for CRP, CRP1 and CRP2, are denoted by pairs of ovals. The △5 and △10 deletions are denoted by a black filled triangle and the +5, +41 and +91 insertions are denoted by a black filled rectangle. For TB28, the substitution of DNA sequences covering sites 1 and 1′ is denoted by a grey bar. (**B**) The figure illustrates β-galactosidase expression in *E. coli* WAM1321 cells carrying *melR* promoter::*lac* fusions, encoded by pRW50 with different EcoRI–HindIII fragments inserted as indicated. β-Galactosidase expression was measured in cells containing pJW15 that encodes MelR (+MelR: black filled bars) or the control pJW*ΔmelR* with no *melR* insert (−MelR: open bars). For each promoter, the activity +MelR is expressed as a% of the activity −MelR. The results are averages from at least three independent determinations.

The electromobility shift assay shows that MelR forms more stable complexes at the TB22 promoter than at the TB28 promoter (Figure 7). With the TB22 fragment, three clear shifted bands are observed. DNAase I footprinting (Figure 8) suggests that these bands are due to the successive occupation of MelR-binding sites 1 and 1′, site 2 and site R. With the TB28 fragment, two weaker bands are seen (Figure 7). DNAase I footprinting shows that these result from MelR binding at site 2 and at site R, and quantification of scans of the gel shows that MelR binding to site R is weakened by at least 2-fold.

In the next experiments, we used AFM to visualize the binding of purified MelR to its targets in the TB22 promoter fragment, to attempt to establish whether DNA loop formation is a feature of the MelR binding. To do this, we exploited an 821-bp SspI–NdeI restriction fragment (Figure 9), which contains the 251-bp TB22 EcoRI–HindIII fragment (Figure 1A) with a short 190-bp extension upstream of the EcoRI site and a longer 380-bp segment downstream from the HindIII site. A mixture containing purified MelR and the DNA fragment was deposited onto a nickel chloride-treated mica surface and imaged by AFM using a cantilever in tapping mode. DNA fragments and MelR–DNA complexes were visualized, and typical examples are shown in Figure 9 (with more examples and data in Figure 2 of the online Supplementary Data). The cluster of the binding sites 2, 1 and 1′ is at a distance from site R that would allow clear visualization of a DNA loop, but no sign of such loops was apparent in any of the ∼100 images of complexes that we examined. Instead, DNA-bound MelR appears as distinct oval foci at a distance of ∼59–64 nm from one end of the DNA fragments. While the length of the shorter DNA arm was approximately the same in all complexes, the length of the longer DNA arm appeared shorter in a third of the complexes. In the examples shown in Figure 9, the longer arm is 205 nm in one complex and 158 nm in the

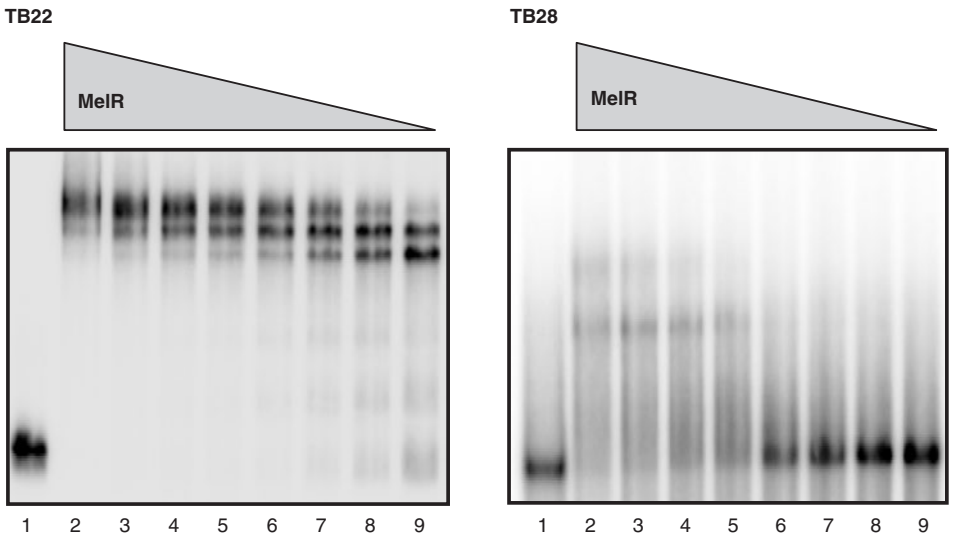

Figure 7. Binding of MelR to the TB22 and TB28 promoter fragments. The figure shows autoradiograms of electromobility shift assays performed with labelled TB22 and TB28 fragments, as indicated, incubated with no MelR (lane 1) or 2000 nM (lane 2), 1000 nM (lane 3), 500 nM (lane 4), 250 nM (lane 5), 125 nM (lane 6), 62.5 nM (lane 7), 31.25 nM (lane 8) and 15.62 nM (lane 9) purified MelR.

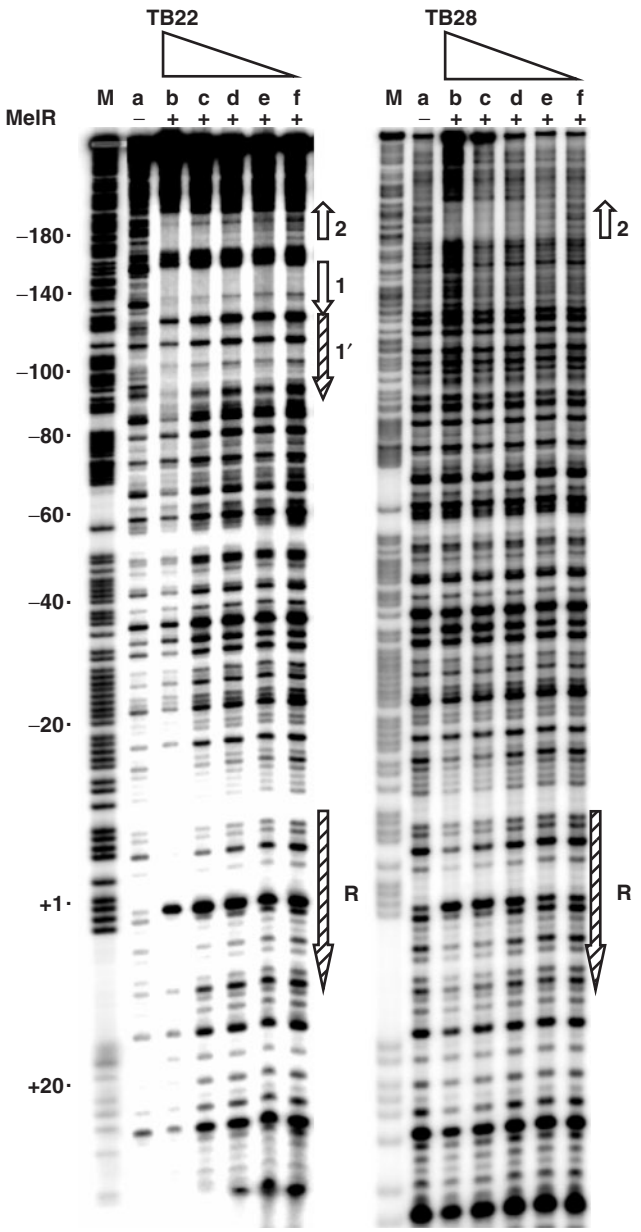

Figure 8. DNAase I footprint analysis of MelR binding. The figure shows an autoradiogram of a sequencing gel on which cleavage of different DNA fragments by DNAase I was analysed. DNA fragments (4 nM), containing the TB22 and TB28 derivatives of the *melR* promoter as indicated, were incubated with purified MelR as follows: lane a, no MelR; lane b, 2000 nM; lane c, 1000 nM; lane d, 500 nM; lane e, 250 nM and lane f, 125 nM. Calibrations with a Maxam–Gilbert G + A reaction are shown in lanes marked M. The calibration is numbered with the *melR* promoter transcript start point taken as +1 and the locations of different DNA sites for MelR are indicated by vertical arrows.

other, and more examples are shown in Supplementary Figure 2. We noticed that the foci due to MelR binding were consistently bigger in the complexes with the shortened arm. In the images shown in Figure 9, the MelR focus is 15×33 nm across the shortest and longest axes of the oval in the complex with the shortened arm (right hand panel), compared to 9×12 nm in the other complex (centre panel). The simplest explanation for these observations, that is consistent with the location of sites in the DNA fragment (Figure 9), is that one type of complex contains 3 MelR molecules bound at sites 2, 1 and 1′ (centre panel), whilst the other contains 4 MelR molecules bound at sites 2, 1, 1′ and R (right panel). Thus there is an apparent progressive shortening of the end-to-end contour length of the DNA from the naked DNA to the MelR-2-1-1′ complex and to the MelR-2-1-1′-R complex. The shortening appears to be due to compaction of the DNA between bound MelR molecules rather than to looping. Note a loop formed from the DNA between MelR bound at sites 2, 1, 1′ and bound at site R would have a diameter of ~13 nm and this is well within the range of sizes visualized in other studies that used the same methodology (29–31).

DISCUSSION

At the *E. coli* arabinose operon regulatory region, transcription is repressed by the binding of two AraC molecules at two targets that are in the same orientation and separated by 210 bp, and a repression loop forms (4,5). Our aim in this work was to ascertain if such a simple model applied to MelR-dependent repression of the *melR* promoter. Our principal conclusion is that optimal repression does require MelR binding at distant targets, but it is more complicated, involving four molecules of MelR.

Expression of the *E. coli* K-12 *melAB* genes, which encode products essential for melibiose metabolism, depends on transcription activation by MelR and CRP, and is triggered by melibiose (7,9). Expression of the *melR* gene depends on transcription activation by CRP, whose activity depends on cyclic AMP (11). In conditions where CRP is active, but melibiose is absent, MelR is made and occupies binding sites 2, 1, 1′ and site R, but it cannot occupy site 2′ and activate the *melAB* promoter, and hence the system is 'poised' (8). In this situation, MelR autoregulates its own expression by binding to site R and repressing its own promoter, and this repression is reinforced by upstream binding of MelR. The simplest model is that repression is dependent on the formation of a complex involving more than one molecule of MelR and we have found that optimal repression requires the binding of MelR at sites R, 2, 1 and 1′, but not the binding of CRP at its targets. Since each target site accommodates one MelR monomer, and since MelR exists in solution as a monomer–dimer equilibrium (Mohamed el-Robh, unpublished data) we suppose that the final repressing complex is a dimer of MelR dimers.

We previously suggested that a MelR dimer simultaneously occupies site R and site 2, creating a repression loop and the effects of different insertions and deletions on MelR-dependent repression of the *melR* promoter (Figure 6) are consistent with this (17). However, we now argue for a repression complex rather than a repression loop, and, taken together, our results suggest that this complex involves MelR bound at sites 1 and 1′, as well as at site 2 and site R. Our AFM imaging data suggest

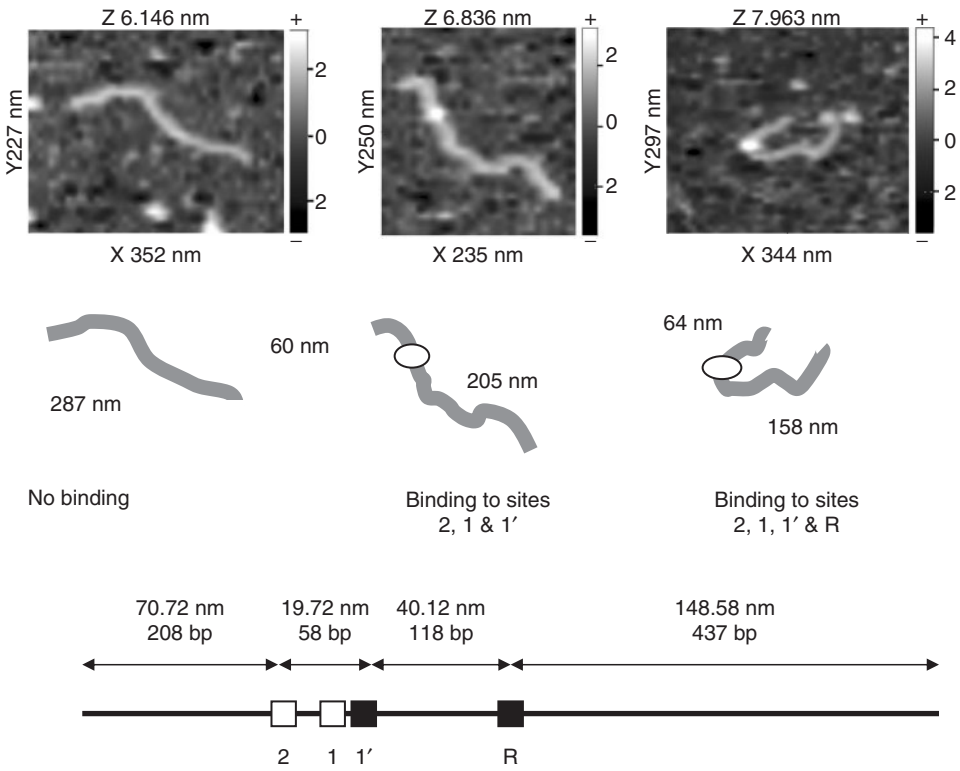

Figure 9. Analysis of MelR binding using AFM. Representative AFM images of the three molecular species observed when purified MelR is incubated with an SspI–NdeI fragment containing the TB22 EcoRI–HindIII fragment (Figure 1A). The images from left to right show naked DNA, and the proposed complexes of MelR bound at sites 2, 1 and 1′, and MelR bound at all four DNA sites 2, 1, 1′ and R. The foci representing the Mel-2-1-1′ (middle) and Mel-2-1-1′-R (right) complexes appear as oval shapes. Precise XYZ dimensions as well as 'heat scales' (in nanometre units) are shown for each scan. Sketches of the different complexes indicating the experimentally measured contour lengths of the DNA molecules are shown below each image. The bottom section of the figure shows a diagram of the SspI–NdeI fragment, indicating the theoretical relative positions of the different binding sites for MelR, assuming 0.34 nm per base pair. In the complexes, DNA regions between the MelR-binding sites are somehow compacted. This results in an apparent shortening of the 'end-to-end' contour length of the DNA fragment from 287 nm in naked DNA to 265 and 222 nm in the Mel-2-1-1′ and Mel-2-1-1′-R complexes, respectively.

that DNA regions between the MelR-binding sites remain associated with the MelR–DNA complexes rather than forced to loop out of the complexes. The nature of this DNA packaging in the MelR–DNA complexes is not clear and might involve MelR-induced DNA bending (32) or wrapping (33), but whatever its nature, the intervening DNA remains accessible to attack by DNAase I (Figure 8). Note that others have argued for repression by complexes rather than by simple loops, and the best example is that of the *E. coli* GalR repressor at the *gal* operon regulatory region, where 'repressomes' have been visualized (29,34). Thus, our results may have implications for understanding the pathway of DNA at other regulatory regions, such as the *E. coli chbB* regulatory region (35,36), where multiple bound factors are required for repression.

SUPPLEMENTARY DATA

Supplementary Data are available at NAR Online.

ACKNOWLEDGEMENTS

This work was supported by the Wellcome Trust, the UK BBSRC and the Darwin Trust of Edinburgh. We thank Stephanie Allen and Clive Roberts for use of the AFM, Georgina Lloyd for providing purified cyclic AMP receptor protein and for advice with *in vitro* transcription experiments, and Christine Webster for excellent technical support. Funding to pay the Open Access publication charges for this article was provided by the Wellcome Trust.

Conflict of interest statement. None declared.

REFERENCES

1. Gralla,J. and Collado-Vides,J. (1996) Organization and function of transcription regulatory elements. In Neidhardt,F. (ed.), *Escherichia coli and Salmonella*, Vol. 1, ASM Press, Washington, DC, pp. 1332–1245.
2. Choy,H. and Adhya,S. (1996) Negative Control. In Neidhardt,F. (ed.), *Escherichia coli and Salmonella*, Vol. 1, ASM Press, Washington DC, pp. 1287–1299.
3. Rojo,F. (2001) Mechanisms of transcriptional repression. *Curr. Opin. Microbiol.*, **4**, 145–151.
4. Schleif,R. (1996) Two positively regulated systems, *ara* and *mal*. In Neidhardt,F. (ed.), *Escherichia coli and Salmonella*, Vol. 1, ASM Press, Washington, DC, pp. 1300–1309.
5. Schleif,R. (2000) Regulation of the L-arabinose operon of *Escherichia coli*. *Trends Genet.*, **16**, 559–565.
6. Gallegos,M-T., Schleif,R., Bairoch,A., Hofmann,K. and Ramos,J-L. (1997) AraC-XylS family of transcriptional regulators. *Microbiol. Mol. Biol. Rev.*, **61**, 393–410.

7. Webster,C., Gardner,L. and Busby,S. (1989) The *E. coli melR* gene encodes a DNA binding protein with affinity for specific sequences located in the melibiose-operon regulatory region. *Gene*, **83**, 207–213.
8. Belyaeva,T., Wade,J., Webster,C., Howard,V., Thomas,M., Hyde,E. and Busby,S. (2000) Transcription activation at the *Escherichia coli melAB* promoter: the role of MelR and the cyclic AMP receptor protein. *Mol. Microbiol.*, **36**, 211–222.
9. Wade,J., Belyaeva,T., Hyde,E. and Busby,S. (2001) A simple mechanism for codependence on two activators at an *Escherichia coli* promoter. *EMBO J.*, **20**, 7160–7167.
10. Webster,C., Kempsell,K., Booth,I. and Busby,S. (1987) Organisation of the regulatory region of the *Escherichia coli* melibiose operon. *Gene*, **59**, 253–263.
11. Webster,C., Gaston,K. and Busby,S. (1988) Transcription from the *E. coli melR* promoter is dependent on the cyclic AMP receptor protein. *Gene*, **68**, 297–305.
12. Michán,C., Busby,S. and Hyde,E. (1995) The *Escherichia coli* MelR transcription activator: production of a stable fragment containing the DNA binding domain. *Nucleic Acids Res.*, **23**, 1518–1523.
13. Kahramanoglou,C., Webster,C., El-Robh,M., Belyaeva,T. and Busby,S. (2006) Mutational analysis of the *Escherichia coli melR* gene suggests a two-state concerted model to explain transcriptional activation and repression in the melibiose operon. *J. Bacteriol.*, **188**, 3199–3207.
14. Tobes,R. and Ramos,J-L. (2002) AraC-XylS database: a family of positive transcriptional regulators in bacteria. *Nucleic Acids Res.*, **30**, 318–321.
15. Martin,R. and Rosner,J. (2001) The AraC transcriptional activators. *Curr. Opin. Microbiol.*, **4**, 132–137.
16. Grainger,D., Belyaeva,T., Lee,D., Hyde,E. and Busby,S. (2003) Binding of the *Escherichia coli* MelR protein to the *melAB* promoter: orientation of MelR subunits and investigation of MelR-DNA contacts. *Mol. Microbiol.*, **48**, 335–348.
17. Wade,J., Belyaeva,T., Hyde,E. and Busby,S. (2000) Repression of the *Escherichia coli melR* promoter by MelR: evidence that efficient repression requires the formation of a repression loop. *Mol. Microbiol.*, **36**, 223–229.
18. Lodge,J., Fear,J., Busby,S., Gunasekaran,P. and Kamini,N-R. (1992) Broad host-range plasmids carrying the *E. coli* lactose and galactose operons. *FEMS Lett.*, **95**, 271–276.
19. Williams,J., Michán,C., Webster,C. and Busby,S. (1994) Interactions between the *E coli* MelR transcription activator protein and operator sequences at the *melAB* promoter. *Biochem. J.*, **300**, 757–763.
20. Grainger,D., Webster,C., Belyaeva,T., Hyde,E. and Busby,S. (2004) Transcription activation at the *Escherichia coli melAB* promoter: interactions of MelR with its DNA target site and with domain 4 of the RNA polymerase σ subunit. *Mol. Microbiol.*, **51**, 1297–1309.
21. Kolb,A., Kotlarz,D., Kusano,S. and Ishihama,A. (1995) Selectivity of the *Escherichia coli* RNA polymerase $E\sigma^{38}$ for overlapping promoters and ability to support CRP activation. *Nucleic Acids Res.*, **23**, 819–826.
22. Perrin,S. and Gilliland,G. (1990) Site-specific mutagenesis using asymmetry polymerase chain reaction and a single mutant primer. *Nucleic Acids Res.*, **18**, 74233–74238.
23. Miller,J. (1972) *Experiments in Molecular Genetics*. Cold Spring Harbor Laboratory Press, Cold Spring Harbor, NY.
24. Caswell,R., Williams,J., Lyddiatt,A. and Busby,S. (1992) Overexpression, purification and characterisation of the *E. coli* MelR transcription activator protein. *Biochem. J.*, **287**, 493–499.
25. Hansma,H., Laney,D., Bezanilla,M., Sinsheimer,R. and Hansma,P. (1995) Applications for atomic force microscopy of DNA. *Biophys. J.*, **68**, 1672–1677.
26. Ishihama,A. (2000) Molecular anatomy of RNA polymerase using protein-conjugated metal probes with nuclease and protease activities. *Chem. Commun.*, **2000**, 1091–1094.
27. Lee,D., Busby,S. and Lloyd,G. (2003) Exploitation of a chemical nuclease to investigate the location and orientation of *Escherichia coli* RNA polymerase alpha subunit C-terminal domains at simple promoters that are activated by the cyclic AMP receptor protein. *J. Biol. Chem.*, **52**, 52944–52952.
28. Meares,C., Datwyler,S., Schmidt,B., Owens,J. and Ishihama,A. (2003) Principles and methods of affinity cleavage in studying transcription. *Methods Enzymol.*, **371**, 82–106.
29. Virnik,K., Lyubchenko,Y., Karymov,M., Dahlgren,P., Tolstorukov,M., Semsey,S., Zhurkin,V. and Adhya,S. (2003) Antiparallel DNA loop in Gal repressosome visualised by atomic force microscopy. *J. Mol. Biol.*, **334**, 53–63.
30. Wang,H., Bash,R., Lindsay,S. and Lohr,D. (2005) Solution AFM studies on human Swi-Snf and its interactions with MMTV DNA and chromatin. *Biophys. J.*, **89**, 3386–3398.
31. Zhang,W., Dillingham,M., Thomas,C., Allen,S., Roberts,C. and Soultanas,P. (2007) Directional loading and stimulation of PcrA helicase by the replication initiator protein, RepD. *J. Mol. Biol.*, **371**, 336–348.
32. Bourgerie,S., Michan,C., Thomas,M., Busby,S. and Hyde,E. (1997) DNA binding and DNA bending by the MelR transcription activator protein from *Escherichia coli*. *Nucleic Acids Res.*, **25**, 1685–1693.
33. Semsey,S., Virnik,K. and Adhya,S. (2005) A gamut of loops: meandering DNA. *Trends Biochem. Sci.*, **30**, 334–341.
34. Roy,S., Dimitriadis,E., Kar,S., Geancopoulos,M., Lewis,M. and Adhya,S. (2005) Gal repressor-operator HU ternary: pathway of repressosome formation. *Biochemistry*, **44**, 5373–5380.
35. Plumbridge,J. and Pellegrini,O. (2004) Expression of the chitobiose operon of *Escherichia coli* is regulated by three transcription factors: NagC, ChbR and CAP. *Mol. Microbiol.*, **52**, 437–449.
36. Kachroo,A., Kancheria,A., Singh,N., Varshney,U. and Mahadevan,S. (2007) Mutations that alter the regulation of the *chb* operon of *Escherichia coli* allow utilisation of cellobiose. *Mol. Microbiol.*, **66**, 1382–1395.